Magnetic island evolution under the action of electron cyclotron current drive

2012 J. Phys.: Conf. Ser. 401 012002

(http://iopscience.iop.org/1742-6596/401/1/012002)

Journal of Physics: Conference Series **401** (2012) 012002 doi:10.1088/1742-6596/401/1/012002

Magnetic island evolution under the action of electron cyclotron current drive

D Borgogno[1], L Comisso[1,2], D Grasso[1,2], E Lazzaro[3]

[1] Dipartimento Energia, Politecnico di Torino, Italy
[2] Istituto Sistemi Complessi - CNR, Roma, Italy
[3] Istituto di Fisica del Plasma "P.Caldirola", Associazione Euratom-ENEA-CNR, Milano, Italy

Abstract. The magnetic island evolution under the action of an externally current generated by electron cyclotron (ECCD) wave beams is studied using a reduced resistive magnetohydrodynamics (RRMHD) plasma model. We found interesting and somewhat unexpected features of the actual nonlinear 2-D evolution of the magnetic perturbation depending on the injection time of the radio frequency control. In particular in the linear phase of the magnetic island growth we observe that the complete annihilation of the island width is followed by a spatial phase shift of the island, referred as "flip"instability. On the other hand, a current drive deposition in the Rutherford regime can be accompained by the occurrence of a Kelvin-Helmholtz type shear flow instability, responsible for the onset of a plasma turbulent behavior.

1. Introduction

In plasma confinement devices the magnetic reconnection process causes a local topological transition of the magnetic surfaces, accompanied by a transformation of magnetic energy into plasma kinetic energy and heat in a short time. In tokamak devices, these tearing modes are a serious cause of degradation of plasma confinement and an important open issue consists of finding the appropriate means of control of this perturbation. Various methods for the mitigation and control of tearing modes have been implemented in existing experiments. One of the most promising methods presently considered to counteract robustly the tearing instabilities in a tokamak is based on the localized injection of an external control current inside the magnetic island [1, 2]. Due to its localized deposition [3], the electron cyclotron current drive (ECCD) is very appropriate for this stabilization purpose, enabling the driven currents to both locally modify the equilibrium [4] and compete with the perturbed island [5]. Experimental results have successfully demonstrated stabilization on several devices [6, 7, 8].

The conventional approach on which practical control systems are being designed is based on the 0-D model of the (generalized) Rutherford equation [9] that describes the time evolution of a nominal width of the island. Although largely applied, in this approach the fundamental topological aspects of the problem are neglected.

In this paper we present numerical results corcerning the effect of ECCD injection on the dynamical behavior of magnetic islands associated with resistive tearing modes, in a fluid plasma. In order to analyze the effect on different size islands, the current drive is turned on at linear, Rutherford and saturated phases of a highly unstable reconnection process. A continuously driven control current peaked at the island O-point has been adopted, whose amplitude is con-

sistent with the magnetic field dynamics.

2. Model and island evolution without current drive

The analysis has been performed by adopting a two-dimensional fluid plasma description based on the standard Reduced Resistive Magneto-Hydro-Dynamics Model (RRMHD). In order to consider the ECCD contribution, an extra term simulating an externally imposed current density source J_{ec} has been added to the plasma Ohm's law. The poloidal magnetic flux function ψ and the vorticity U evolution equations are [10]:

$$\frac{\partial \psi}{\partial t} + \mathbf{v}_\perp \cdot \nabla \psi = -\eta (J - J^{(0)} + J_{ec}), \tag{1}$$

$$\frac{\partial U}{\partial t} + \mathbf{v}_\perp \cdot \nabla U - \mathbf{B}_\perp \cdot \nabla J = 0 \tag{2}$$

The total magnetic field is $\mathbf{B} = B_0 \mathbf{e}_z + \mathbf{B}_\perp$, the in-plane magnetic field is $\mathbf{B}_\perp = \nabla \psi \times \mathbf{e}_z$, the in-plane velocity is $\mathbf{v}_\perp = -\nabla \varphi \times \mathbf{e}_z$ and $U = \mathbf{e}_z \cdot (\nabla \times \mathbf{v}_\perp) = \nabla_\perp^2 \varphi$, where φ is the stream function. The current density is $J = \mathbf{e}_z \cdot (\nabla \times \mathbf{B}_\perp) = -\nabla_\perp^2 \psi$ and $J^{(0)}$ is its equilibrium component. The parameter η represents the plasma resistivity, which corresponds to the physical effect responsible for the decoupling between the magnetic surfaces and the plasma motion and, as a consequence, for the triggering of the magnetic reconnection instability. All lengths are scaled to the macroscopic scale length L, while the time is normalized by the Alfvén time $\tau_A = L/B_y^{(0)}$, with $B_y^{(0)}$ the characteristic value of the equilibrium magnetic field in the perpendicular plane and L its shear length.

The control density current is assumed to have the following spatial gaussian form

$$J_{ec}(x, y, t) = J_m(t) exp(-(\psi(x, y, t) - \psi_O(t))^2/\delta^2), \tag{3}$$

where ψ_O is the magnetic flux at the O-point of the magnetic island. This allows a uniform distribution of the control current on the magnetic surfaces $\psi = const$. The aim of an auxiliary driven control current like eq.(3) is to restore the ideal frozen flux condition in eq.(1), by reducing the perturbed current density $J - J^{(0)}$. It is expected to counterbalance the unstable reconnection process and eventually to stop the magnetic island growth [11, 12, 13].

The maximum height J_m has a step function profile like

$$J_m(t) = \begin{cases} 0 & t < t_1 \ V \ t > t_2 \\ A & t_1 < t < t_2 \end{cases} \tag{4}$$

where t_1 and t_2 are the switching on and switching off time of the current control, respectively. The amplitude A is a constant proportional to the difference between the maximum and the minimum current density value along the rational surface $x = x_s$ at $t = t_1$, $A = a \cdot (J_{max}(t_1) - J_{min}(t_1))$. Finally, δ is a constant, representing the EC beam width in ψ space, and taken proportional to the difference between the magnetic flux at the X- and the O-point of the magnetic island when $t = t_1$, i. e. $\delta = b \cdot (\psi_X(t_1) - \psi_O(t_1))$.

The equations (1)-(2) are integrated numerically by splitting all the fields in two parts: an equilibrium, independent on time, and an evolving perturbation. The perturbed component is advanced in time by an explicit, fourth order Adam-Bashforth scheme. The equations are solved in a $L_x \times L_y$ slab, with periodic boundary conditions along the y direction. Dirichlet conditions are applied at the edges of the x axis, imposing that all the perturbed fields go to zero. A compact finite difference algorithm [14], suitable for non-equispaced grid, is used for the spatial

operations along the x direction, while pseudo-spectral methods are adopted for the periodic direction. Numerical filters are introduced in order to control the numerical error propagation. As described in [14], these filters smooth out the small spatial scales below a chosen cutoff, while leaving unchanged the large scale dynamics on all the time evolution of the process. In order to address the proper spatial resolution to have a reasonably good scale separation in the simulations, the code has been parallelized adopting the MPI libraries.
We set up a numerical experiment of spontaneous magnetic reconnection process in a static, "Harris pinch" equilibrium configuration with

$$B_{\perp y}^{(0)} = B_y^{(0)} \tanh(x/L) \qquad \text{and} \qquad \mathbf{v}_\perp^{(0)} = 0, \tag{5}$$

where $B_y^{(0)} = 1$ and $L = 1$. The linear theory shows that this equilibrium becomes tearing mode unstable if the instability parameter $\Delta' = 2 \cdot (1/k_y - k_y) > 0$, where $k_y = 2\pi m/L_y$ is the instability wave number along y, m being the corresponding mode number [15]. In this analysis we considered $L_y = 8\pi$, which corresponds to a rather large value of $\Delta' = 7.5$ for $m = 1$. It is accepted that in the regimes $\Delta' \gg 1$ magnetic reconnection can develop on a relatively fast time scale both in collisional [16] and collisionless [17, 18, 19] regimes. Moreover there is experimental evidence for $\Delta' \gg 1$ during the sawtooth instability (see, e.g., [20] and references therein). The box extention along the x direction is $L_x = 22.64$, which avoids any influence of boundary conditions on the reconnection dynamics. We destabilized the equilibrium (5) by introducing the following current density perturbation

$$\delta J(x, y) = \hat{J}(x) cos(k_y y), \tag{6}$$

where $k_y = 1/4$ and $\hat{J}(x)$ is a function localized within a width of order $(\eta/k_y)^{1/3}$ around the rational surface $x_s = 0$, whose amplitude is 10^{-4}. We assumed a plasma resistivity $\eta = 5 \cdot 10^{-4}$. In order to properly treat the small scale structures we expect in the large Δ' regime [16], a mesh of $nx = ny = 1024$ grid points has been adopted.
The time evolution of the reconnection process we considered is shown in fig.1. The figure describes the variation of the magnetic island width when the current control is switched off ($J_{ec} = 0$), through the logarithmic plot of the magnetic flux function at the X-point versus the time.

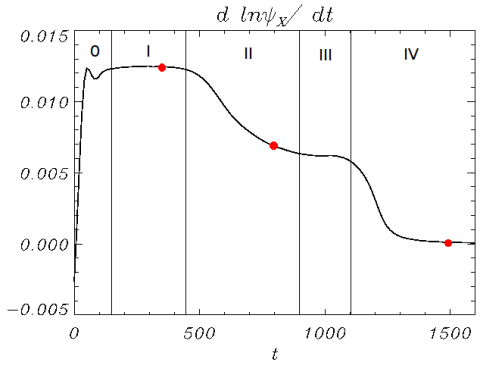

Figure 1. Effective growth rate at the X-point vs time for the free evolving system. After the initial transient (0), four main stages can be identified: the linear exponential growth (I), the Rutherford regime (II), the second exponential phase (III) and finally the saturation (IV). The red dots indicate the instants at which the current drive has been switched on.

After a short transient, four distinct stages can be identified. In the time interval $150 < t < 450$ the single helicity magnetic perturbation exhibits a linear exponential growth in time [21]. Then at $t = 500$ the Rutherford regime starts, lasting till $t = 900$, during which the magnetic island growth is algebraic in time [22]. Note that in the case we present here, the Rutherford

stage does not lead to the saturation regime, as predicted by the resistive MHD for $\Delta' \ll 1$. Indeed, a second exponential growth starts around $t = 900$ and it lasts till $t = 1100$. Contrary to the simulations with large Δ' reported in [16, 23], no collapse of the cross shape current configuration, centered at the X-point of the island, develops at this stage as well as current sheet formation. The disagreement depends on the characteristic Δ' value of the initial equilibrium configuration we considered. Even though we analyzed a strongly driven tearing mode, the value of Δ' is not large enough to satisfy the analytical Waelbroeck's transition criterion [24], which predicts the current sheet collapse when the magnetic island width W is larger than the threshold value W_c, with $W_c = 25/\Delta'$. Indeed, in our case the magnetic island width at the $t = 1000$, when the collapse is expected, is $W \approx 3.23$ which is slightly lower than $W_c \approx 3.33$. Finally, at $t = 1100$ the magnetic island growth rate falls quickly down and at $t = 1300$ the island width saturates.

3. Effect of current drive with gaussian profile on the island width

In order to analyze the influence of an externally driven current control on the magnetic island, we applyed the current drive J_{ec} in the linear, Rutherford and saturated phase of the reconnection process described in the previous section. In all the cases we explored the J_{ec} parameters lay in the intervals $1 < J_m/(J_X - J_O)|_{t_1} < 10$ and $0.1 < \delta/(\psi_X - \psi_O)|_{t_1} < 1$, where J_X and J_O represent the current density at the X and at the O-point of the magnetic island, respectively. The basic response of the tearing mode perturbation to the injection of the electron cyclotron (EC) driven current is monitored by the time history of the effective area $A_{isl}(t)$ enclosed by the separatrix of the magnetic island. The island contour is found identifying numerically the cordinates of the hyperbolic X-point, (x_X, y_X), where $\partial_x\psi = \partial_y\psi = 0$, and tracking accurately the surface level $\psi(x, y, t) = \psi(x_X, y_X, t)$, whose area A_{isl} is calculated.

Fig.2 shows the evolution of the area of a linear, small size magnetic island, after the injection of the current density J_{ec} at $t_1 = 350$. The left frame displays several $A_{isl}(t)$ traces corresponding to different values of the shine-on spot δ, for a fixed value of the amplitude $J_m = 4 \cdot (J_X - J_O)|_{t_1}$, J_X and J_O being the current density values at the hyperbolic and elliptic point of the magnetic island respectively. It is apparent that the dependence of $A_{isl}(t)$ on δ is strongly nonlinear. The optimum control corresponds to the absorption depth $\delta = 0.5 \cdot (\psi_X - \psi_O)|_{t_1}$. In this case, after a short transient in which the island slightly grows, its area falls rapidly to zero, in the limit of the numerical precision we assumed, in a time interval comparable to the linear growth time of the free system, $\gamma_{lin}^{-1} \sim 1/0.012$. Lower values of δ allow a very poor control on the magnetic island growth mainly because they are too small compared to the original island size. On the other hand, when $\delta = (\psi_X - \psi_O)|_{t_1}$ we numerically verified that almost the 20% of the externally imposed ECCD is deposited ouside the magnetic island at $t = 350$ and, as a consequence, does not contribute to the island reduction. This is responsible for the lower rate of quench compared to the case with $\delta = 0.5 \cdot (\psi_X - \psi_O)|_{t_1}$. By varying the current drive amplitude we observed that no significant control can be reached for $J_m < 4 \cdot (J_X - J_O)|_{t_1}$ for any $0.1 < \delta/(\psi_X - \psi_O)|_{t_1} < 1$. On the contrary, when $J_m > 4 \cdot (J_X - J_O)|_{t_1}$ the auxiliary control current is suitable to counteract significantly the current pertubation growth due to the tearing mode instability. In this case the magnetic island annihilation is reached on a time scale that decreases monotonically with the inverse of the current drive amplitude.

As shown in the right frame of fig.2, a remarkable fact occurs for a critical value $\delta = 0.5 \cdot (\psi_X - \psi_O)|_{t_1}$ at later times. After the suppression at $t = 550$, the area of the island bounces back with a growth rate equal to the previous rate of quench. In other words the effect of the applied current meant to restore stability in the linear stage (so called "early" control action) may lead on the contrary to another unstable state. This is a state bifurcation known as *flip* instability [25, 26] because the value of the reconnected flux ψ at the resonant surface

changes sign, which is equivalent to a shift of $L_y/2$ of the equilibrium position of the elliptic O-point of the tearing perturbation. It is noteworthy that this behaviour, already studied in the context of classical reconnection driven by perturbation of boundary conditions reappears, with universal chacteristics, in the frame of the so-called non-inductive current drive effects where it has been always ignored. The consequences of this effect on the strategy of control of tearing instabilities can be better appreciated inspecting also the 2D structure of the islands before, during and after the ECCD injection.

The effect of the localized current injection on a macroscopic magnetic island in the Rutherford

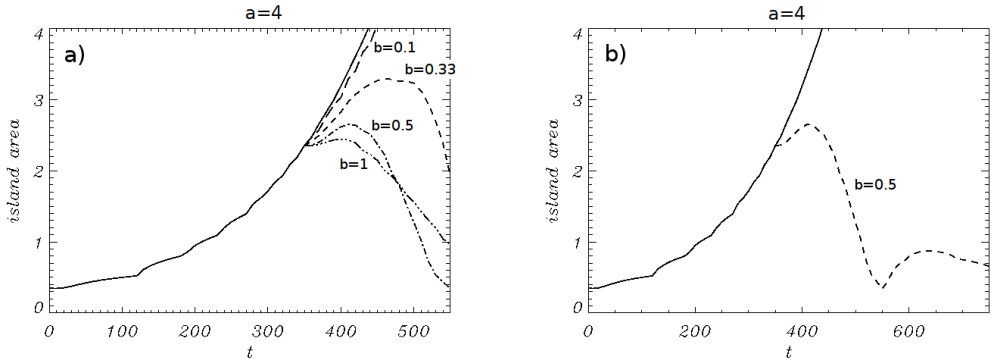

Figure 2. (a) Time evolution of the magnetic island area for four different values of the normalized current drive width $b = \delta/(\psi_X - \psi_O)|t_1$. The control current source has been switched on at $t = 350$ with a maximum height of $J_m = 4 \cdot (J_X - J_O)|t_1$. (b) In the case $b = \delta/(\psi_X - \psi_O)|_{t_1} = 0.5$, once the magnetic island reaches a sufficiently small size the island reverts back to instability. The actual cause of the abrupt change is the result of a phase shifted island being driven by the radio frequency current. We refer to this behavior as *flip* instability.

regime has been investigated by turning on J_{ec} at $t_1 = 800$. A characteristic feature of the system in this phase, as was already shown in recent research works [13, 28], is that the island suppression process does not proceed on a reversible path through a gradual shrinking of the island size and a restoration of a state similar to the initial one. An alternative equilibrium is reached with two straight, thin and parallel to the y axis current sheets symmetrically distributed on both sides of the resonant surface $x_s = 0$. The current layers are localized around the maximum width of the magnetic island at $t = 800$, independently from the strength and the width of the current drive. In [27] an interpretation of this behavior is found by analogy with the classical Hahm-Kulsrud-Taylor problem [29, 30]. An exemple of the plasma current distribution, in response to the EC driven current pulse with parameters $J_m = 4 \cdot (J_X - J_O)|t_1$, $\delta = 0.5 \cdot (\psi_X - \psi_O)|_{t_1}$, exhibiting the formation of a twin current sheet structure is shown in fig.3.

Numerical simulations have shown that the complete suppression of the magnetic island in the Rutherford regime is more difficult than in the linear stage. It occurs just for a rather narrow range of combinations of the J_{ec} parameters, on much longer time scales than the ones observed in the linear island control case. As an example, fig.4 shows the evolution of magnetic island area for different values of δ and a fixed $J_m = (J_X - J_O)|_{t_1}$.

The new nonlinear equilibrium has shown to be prone to secondary instabilities. The current sheet formation is coupled to highly localized, bar shaped, vorticity structures giving rise to strong shears that lead to the onset of fluid like, Kelvin-Helmholtz instabilities. The vorticity layers are aligned to the y axis and picked around the current sheet positions, where $\mathbf{B}_\perp \sim B_y$ and $\partial_y J \sim 0$. As a consequence the contribution of the nonlinear term $\mathbf{B}_\perp \cdot \nabla J$ in the equa-

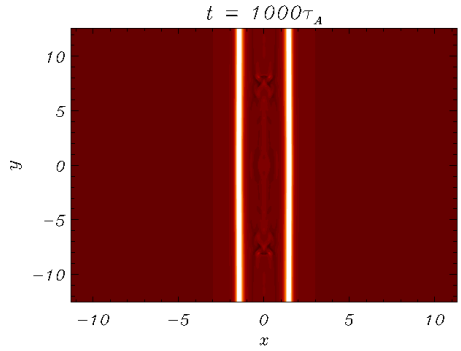

Figure 3. Contour plot of the current density J at $t = 1000$ in response to the ECCD pulse turned on in the Rutherford regime ($t_1 = 800$).

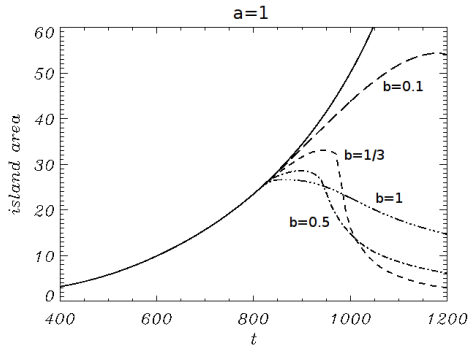

Figure 4. Time evolution of the magnetic island area for control current injections at $t_1 = 800$, with various normalized EC beam widths $b = \delta/(\psi_X - \psi_O)|t_1$ and a fixed maximum height $J_m = (J_X - J_O)|_{t_1}$

tion (2) is almost negligible, wich makes the vorticity evolution almost completely fluid. The Kelvin-Helmholtz like secondary instability is responsible for the turbulent redistribution of the patterns in the spatial region confined by the current layers. It affects not only the fluid field, but also the magnetic field, whose surfaces are advected by the turbulent motion towards the resonant surface $x = 0$, forcing them to reconnect. According to the recent results that highlighted the role of the turbulence on the enhancement of the reconnection rate [31, 32], the generation of the Kelvin-Helmholtz instability could represent a strong limitation for the efficiency of the control startegy. Fig.5 shows the evolution of the vorticity structures in presence of the Kelvin-Helmholtz instability at four different stages of a numerical simulation with external control of parameters $J_m = 3 \cdot (J_X - J_O)_{t_1}$, $\delta = 0.1 \cdot (\psi_X - \psi_O)|_{t_1}$.

In order to analyze the effect of an ECCD power deposition on a tearing mode at the nonlinear saturation stage we carried out a campaign of numerical simulations where the external current control has been injected at the instant $t = 1500$ of the free system evolution. Compared to the control in the linear and in the Rutherford phase, in this case the magnetic island never shrinks to zero. A new equilibrium is reached on a time scale comparable to the time the free system takes to reach the magnetic island saturation, with two current sheets on each side of the singular $x = 0$ surface and a macroscopic deformation of the magnetic topology.

The ECCD control models of tearing modes based on the conventional 1-D Rutherford equation predict very stringent requirements of the focusing of the EC wave beam on the magnetic island. The present study which includes finite 2-D nonlinear effects shows that a successful control action requires broader current deposition, less demanding from the control point of view. However a broader ECCD deposition causes a rapid fall of the control efficiency, due to the fact that a relevant fraction of the injected current falls outside the separatrices, even in presence of small magnetic island reduction.

4. Conclusion

The results of the detailed 2-D nonlinear dynamics of tearing modes under the action of a finite width EC wave beam allow an improved understanding of the role of effects occurring on different space scales, such as the beam width, the island width and the shielding current sheets. When the ECCD is applied to a large size island, in particular, these effects strongly change the

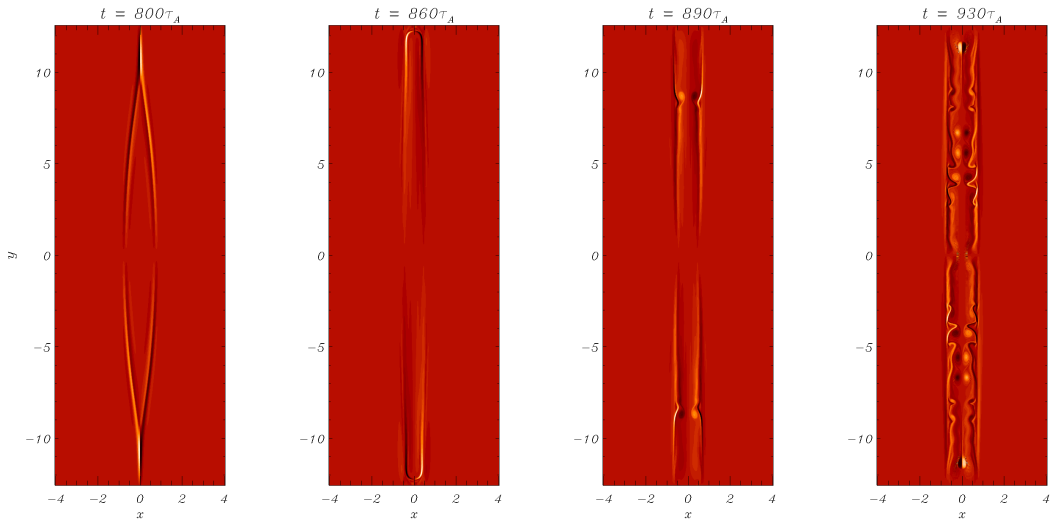

Figure 5. Nonlinear evolution of the vorticity patterns in response to the radio frequency power current drive injection at $t_1 = 800$.

perturbation spectrum, with the apperance of secondary harmonics and the modification of the original magnetic equilibrium, which reduce the control action, designed specifically for decreasing the primary, most unstable armonic. These effects are different from those of conventional Rutherford models and should be considered carefully in practical applications.

5. Acknowledgments

This work was partly supported by the Euratom Communities under the contract of Association between EURATOM/ENEA. The views and opinions expressed herein do not necessarily reflect those of the European Commission.

References

[1] Lazzaro E and Nowak S, *Plasma Phys. Control. Fusion*, **51**, 035005, (2009).
[2] Zohm H, *Phys. Plasmas*, **4**, 3433 (1997).
[3] Fisch J, *Rev. Mod. Phys.*, **59**, 175 (1987).
[4] Pletzer A and Perkins F W, *Phys. Plasmas*, **6**, 1589 (1999).
[5] Hegna C and Callen J D, *Phys. Plasmas*, **4**, 2940 (1997).
[6] Gantenbein G et al., *Phys. Rev. Lett.*, **85**, 1242 (2000).
[7] Maraschek M et al., *Phys. Rev. Lett.*, **98**, 025005 (2007).
[8] Goodman T P et al., *Phys. Rev. Lett.*, **106**, 245002 (2011).
[9] La Haye R J, *Phys. Plasmas*, **13**, 055501 (2006).
[10] Strauss H R, *Phys. Fluids*, **19**, 134 (1976).
[11] Prater R, *Phys. Plasmas*, **11**, 2349 (2003).
[12] Woodby J, Schuster E, Bateman G, Kritz A H, *Phys. Plasmas*, **15**, 092504 (2008).
[13] Comisso L, Lazzaro E, *Nucl. Fusion*, **50**, 125002 (2010).
[14] Lele S K, *J. Comp. Phys.* **103**, 16 (1992).
[15] Biskamp D, *Magnetic Reconnection in Plasmas*, Cambridge University Press 2000.
[16] Loureiro N F, Cowley S C, Dorland W D, Haines M G and Schekochihin A A, *Phys. Rev. Lett.*, **95**, 235003 (2005).
[17] Aydemir A Y, *Phys. Fluids B*, **4**, 3469 (1992).
[18] Ottaviani M and Porcelli F, *Phys. Rev. Lett.*, **71**, 382 (1993).

[19] Kleva R G, Drake J F and Waelbroeck F L, *Phys. Plasmas* **2**, 23 (1995); Wang X and Bhattacharjee A, *Phys. Rev. Lett.* **70**, 1627 (1993).
[20] Angioni C et al., *Plasma Phys. Control. Fusion*, **44**, 205 (2002).
[21] Furth H P, Killen J, Rosenbluth M N, *Phys. Fluids*, **6**, 459 (1963).
[22] Rutherford P H, *Phys. Fluids*, **16**, 1903 (1973).
[23] Jemella B D, Shay M A, Drake J F, Rogers B N, *Phys. Rev. Lett.*, **91**, 125002 (2003).
[24] Waelbroeck F L, *Phys. Rev. Lett.*, **70**, 3259 (1993).
[25] Monticello D A, White R B, Rosenbluth M N, Plasma Physics and Controlled Nuclear Fusion Research 1978, *Proc. 7th IAEA Int, Conf. Tokyo*, 1978, paper IAEA-CN- 37/K-3, Vol. 1, Vienna, p. 605.
[26] Lazzaro E, Coelho R, *Eur. Phys. J. D* **19**, 97 (2002).
[27] Lazzaro E, Comisso L, *Plasma Phys. Control. Fusion*, **53**, 054012 (2011).
[28] Lazzaro E, Comisso L, Valdettaro L, *Phys. Plasmas*, **17**, 052509 (2010).
[29] Kulsrud R M and Hahm T S, *Phys. Scr.*, **T2B**, 525 (1982).
[30] Hahm T S and Kulsrud R M, *Phys. Fluids*, **28**, 2412 (1985).
[31] Loureiro N F, Uzdensky D A, Schekochihin A A, Cowley S C and Yousef T A, *Mon. Not. R. Astron. Soc.*, **399**, L146 (2009).
[32] Lapenta G, *Phys. Rev. Lett.*, **100**, 235001 (2008).